HiSST: 3rd International Conference on
High-Speed Vehicle Science Technology
14 -19 April 2024, Busan, Korea

Direct numerical simulation study on pressure amplification and shock-boundary layer

Yujoo Kang[1], Sang Lee[2]

Abstract

In the present study, a direct numerical simulation (DNS) of a shock boundary layer interaction injected with a freestream flow of M = 2.9 over a 24° compression ramp is performed to investigate the pressure response within and posterior to the interaction region. The rise in the pressure is inherent due to the shock compression. However, the increase in the pressure fluctuation is a complex process in which the augmented turbulence plays a dominant role due to the second phase flow deflection. With the lack of understanding at present, a DNS is performed to characterize the interaction and the downstream zone.

Keywords: Shock-turbulent boundary layer interaction, direct numerical simulation, shock separation

Nomenclature

u – Streamwise velocity component
p – Pressure
ρ – Density
M – Mach number
T – Temperature
Cf – Skin friction coefficient
δ – Boundary layer thickness
θ – Momentum thickness

Superscripts
- – Reynolds averaging operator

Subscripts
0 – Parameters at reference station
w – Wall parameters
` – Fluctuation

1. Introduction

The origins of the low-frequency unsteadiness observed in shock-induced turbulent separation within turbulent boundary layer flow configurations has been investigated for several decades with a lack of unified conclusion. Despite considerable research efforts, numerous unresolved inquiries persist, particularly concerning the dynamic interplay of unsteady effects precipitated by interactions where the imposition of an adverse pressure gradient by the shock culminates in boundary-layer separation. Empirical observations and computational analyses in canonical Shock Boundary Layer Interactions (SBLI), including scenarios such as compression ramps, impinging oblique shocks, blunt fins, and forward-facing steps, uniformly corroborate the presence of broadband low-frequency shock motions. However, the precise mechanistic underpinnings governing the temporal dynamics of separation remain unsolved.

The delineation of mechanisms driving low-frequency, large-scale shock oscillations has emerged as a principal research thrust over the past two decades, primarily due to the formidable challenges posed to numerical simulations, particularly within the framework of Reynolds-averaged Navier-Stokes methods. Acknowledging the inherent limitations of such computational approaches, recent investigations have increasingly turned to Direct Numerical Simulation (DNS) and Large-Eddy Simulation (LES) methodologies, yielding noteworthy advancements in understanding as reported in Pirozzoli and

[1] *Korea Advanced Institute of Science and Technology, Daejeon, South Korea, ky5731@kaist.ac.kr*
[2] *Korea Advanced Institute of Science and Technology, Daejeon, South Korea, slee1@kaist.ac.kr*

Grasso [1] and Touber and Sandham [2, 3]. In the scientific literature, numerical studies with sufficiently extended integration times capable of investigating low-frequency unsteadiness are notably scarce. For instance, DNS outcomes reported by Pirozzoli and Grasso [1] spanned an integration period of merely 25 units based on freestream velocity and the boundary layer thickness. Addressing this gap, Priebe et al. [4] undertook DNS analysis of a Mach 2.9 impinging SBLI at a Reynolds number of 10^3 and a deflection angle of 12 degrees, closely mirroring the experimental conditions detailed by Bookey et al. [5]. Their comprehensive simulation, extending over approximately 800 units, specifically delved into the low-frequency dynamics characterizing the interaction.

However, a direct comparison with experimental unsteady measurements remains absent. Notably, Touber and Sandham [2] emerged as pioneers, likely being among the first to present a successful alignment between their extensive, long-term narrow-domain LES findings and empirical data concerning the unsteady shock motion. Subsequent to their groundbreaking work, a series of LES investigations focusing on the low-frequency aspects of impinging SBLI phenomena have been documented in Pasquariello et al. [6] and Nichols et al. [7].

Nevertheless, the majority of these investigations primarily concentrated on scenarios involving weak interactions, characterized by the absence of a distinct pressure plateau within the separated flow with low Reynolds numbers typically below Reynolds number of 10^3. High Reynolds number compression corner experiments conducted by Dolling and Or [8] have demonstrated that the wall-pressure signal proximal to the separation-shock foot exhibits high intermittency, primarily reflecting the inviscid pressure jump across the oscillating shock. In studies focusing on low Reynolds numbers, it has been observed that the reflected shock foot does not penetrate as deeply into the boundary layer compared to that of higher Reynolds numbers. This reduced penetration is attributed to increased viscous effects, which diffuse the separation-shock foot into a compression fan. Consequently, this phenomenon leads to a broader range of frequencies with attenuated shock intermittency, as outlined by Ringuette et al. [9]. While the diverse characteristics of shock motion discussed are intriguing, it is essential to recognize that the motions of separation shocks are fundamentally influenced by the unsteadiness of the separated flow. Historically, investigations have largely bifurcated into two perspectives: attributing the low-frequency unsteadiness either to upstream turbulent boundary layer forcing or to an intrinsic instability inherent to the separated flow dynamics.

2. Low Frequency Source

In early experimental endeavors, Andreopoulos and Muck [10] were pioneers in establishing a direct correlation between the bursting events occurring in the incoming turbulent boundary layer and the subsequent motions of shock waves in their Mach 3 compression ramp flow. Similarly, Erengil and Dolling [11] observed a direct response of the reflected shock to fluctuations in upstream pressure, albeit manifesting as high-frequency, smaller-scale jitter motions that did not fully account for the observed large-scale, low-frequency oscillations. Subsequent to these experimental findings, Adams [12] conducted a DNS of a Mach 3 compression ramp flow, revealing a close proximity between the bursting frequency and the shock-crossing frequency, thereby reinforcing the earlier observations made by [10].

Unalmis and Dolling [13] postulated that a low-frequency thickening and thinning of the upstream turbulent boundary layer induces an upstream and downstream motion of the shock. Subsequently, Beresh et al. [14] employed particle image velocimetry (PIV) to substantiate this proposition. Their investigation confirmed that the upstream conditionally averaged velocity profiles exhibited greater fullness when the shock foot was positioned downstream, and conversely, when it was positioned upstream. Furthermore, utilizing time-resolved PIV on a streamwise–spanwise plane and applying Taylor's hypothesis, Ganapathisubramani et al. [15] identified the persistence of low-velocity fluid upstream of their compression ramp flow, maintaining coherence for approximately 50 boundary-layer thicknesses. The investigation conducted by Ganapathisubramani et al. [15] revealed a robust correlation between the identified "superstructures" and an instantaneous surrogate for separation line location. From their findings, they inferred that the transit of these superstructures plays a pivotal role in generating the observed low-frequency unsteadiness within their interaction framework. In contrast, Wu and Martín [16] reported a lack of significant low-frequency correlation between the actual separation point and the upstream turbulent structures in their DNS analysis of a Mach 2.9 compression ramp study. However, the authors identified a spanwise wrinkling of the shock characterized by high-

frequency and small amplitude, which exhibited correlation with the mass flux within the incoming turbulent boundary layer. Simultaneously, through the application of tomographic PIV to an impinging SBLI at Mach 2.1, Humble et al. [17] observed that the traversal of upstream coherent structures led to the development of spanwise wrinkling in the shock foot. This spanwise variation will be further discussed in the subsequent section.

The investigation reveals amplification of Reynolds shear stress and turbulence within the shock region. Notably, observations include boundary-layer separation at the shock impingement point and low-frequency unsteady shock movements. Significant experimental contributions to this field include the compression corner study conducted by by Ringuette et al. [9]. The proposition of upstream elongated structures within the boundary layer and their association with the large-scale instability induced by shock-induced flow separation emerges as a prominent hypothesis regarding the primary source of shock unsteadiness.

A numerical investigation by Wu and Martin [16], uncovered robust correlations between upstream structures and the low-frequency unsteadiness of shock position. Notably, Pirozzoli and Grasso [1] identified the cause of increased turbulent kinetic energy (TKE) and low-frequency shock unsteadiness as the interaction between incoming structures in the upstream boundary layer and the incident shock tip. Furthermore, Pirozzoli et al. [18] observed an intermittent transitory detachment within the interaction region, characterized by scattered instances of instantaneous flow reversal.

Theories falling within the second category establish a link between the motion of the separation shock and mechanisms originating downstream of it, thereby connecting the dynamics of the separation bubble to the unsteady movements of the shock. This concept finds its roots in early experimental observations by Dolling and Erengil [19], and Thomas et al. [20] concerning compression ramp configurations. More recent investigations by Dupont et al. [21] have extended this theory to impinging SBLI.

These investigations have revealed that wall-pressure fluctuations, assessed in proximity to the shock foot and nearing reattachment, exhibit correlations at frequencies linked to the motion of the separation shock. Notably, the observed phase shift suggests a periodic expansion and contraction of the separation bubble. Furthermore, through the analysis of conditionally averaged PIV velocity fields corresponding to small and large bubbles, Piponniau et al. [22] observed that the position of the reflected shock tends to be situated further downstream and upstream, respectively. They postulated a self-sustaining mechanism to explain the low-frequency shock motions, predicated on the entrainment of fluid by the shear layer formed downstream of the reflected shock, positioned above the enclosed separation bubble. Wu and Martin [16] proposed a comparable entrainment-recharge mechanism, positing a feedback loop involving the separation bubble, the detached shear layer, and the shock system.

Pirozzoli and Grasso [1] undertook a brief-duration DNS of a Mach 2.25 impinging SBLI, suggesting an acoustic feedback mechanism as a potential catalyst for low-frequency unsteadiness. Their hypothesis posits that shear-layer vortices, interacting with the incident-shock tip, produce acoustic disturbances that propagate upstream through the subsonic layer, subsequently prompting an oscillatory motion of the separation point. Touber and Sandham [6] linear-stability analysis of the mean flow unveiled a two-dimensional globally unstable mode, suggesting a potential linkage to the low-frequency unsteadiness observed in the system.

Building upon the Navier–Stokes equations and integrating insights from LES outcomes, Touber and Sandham [6] derived a stochastic ordinary differential equation governing the low-frequency motions of the shock foot. Remarkably, the final formulation closely resembled the mathematical framework posited by Plotkin [23]. Furthermore, they advanced the argument that the low-frequency unsteadiness represents an inherent low-pass filter effect stemming from the interaction, rather than being solely an externally imposed property resulting from upstream or downstream forcing. Nevertheless, they emphasized that some form of coherent or incoherent (white noise) forcing at low frequencies is essential for the manifestation of low-frequency shock oscillations in the system.

Drawing from divergent findings across numerous studies regarding the origin of low-frequency shock motions, Clemens and Narayanaswamy [24] and Souverein et al. [25] posited that both mechanisms, upstream and downstream, are likely at play, contingent upon the state of the SBLI. In the present study, DNS simulations have been performed to seek the physical insight to the fluid physics the occur within the core of the SBLI.

3. Numerical Method

The direct numerical simulation solves the unsteady compressible Navier-Stokes equations which employs the molecular viscosity calculated from the Sutherland's law assuming ideal gas. A sixth-order compact finite difference and a third-order Runge-Kutta schemes are employed spatial differentiation and temporal integration to solve the fluid equation. A modified Durcros-type sensor is used to detect shocks which activates the second-order low-pass filter [26] to ensure numerical stability. In addition, artificial diffusivity by Kawai and Lele [27] is employed to stabilize the high-frequency numerical oscillations that are inherently present in shock related flows. With an incoming flow of M=2.9, the turbulent tripping method of Porter and Poggie [28] is used in the present study to generate the turbulent boundary layer flow. The inflow conditions are provided in Table 1. The numerical details are described in Kang and Lee [29].

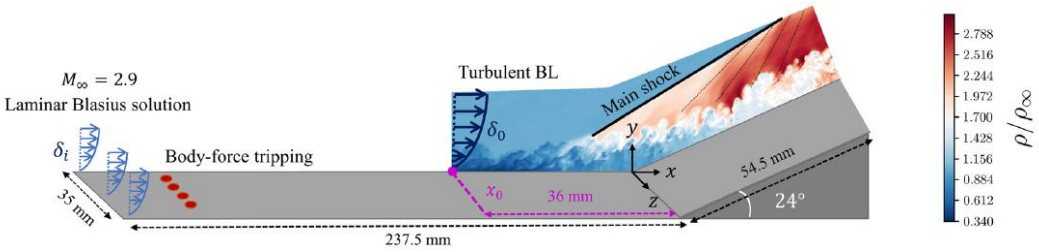

Fig. 1 Computational domain schematic

Table 1. Inflow conditions

Case	Ma_∞	T_∞ (K)	T_w (K)	δ_0 (mm)	θ_0 (mm)	Re_θ	C_f
Bookey *et al.*[24]	2.9	107.1	307	6.7	0.43	2400	0.002 25
Present DNS	2.9	107	307	6.7	0.43	2400	0.002 27

4. Result

Streamwise velocity plot in a wall-parallel plane shows that, at the viscous sublayer, elongated streaks breakdown past the shock impingement point which dissipate in the reattachment region further downstream. This can be quantified by the shear rate parameter. In general, the low-speed streaks come into appearance when turbulence production due to mean shear exceeds the viscous dissipation, as shown in Fig. 2. Upstream of the shock interaction region, elongated streaky vortical structures dominate the flow in the boundary layer. In addition, changes to the turbulent eddy structures are observed as their streamwise length is compressed while the transverse length is expanded, similar to the results report by Kang and Lee [29]. The causes of these geometric changes are still unclear. Wu and Martin [16] attribute the causes to one of two theories, either 1) a chopping mechanism by the shock wave or 2) the adverse pressure gradient. The onsets of larger coherent structures, which are generally associated with low pressure cores, can also be a major cause of large-scale unsteadiness. In particular, the distortions of the eddy structure can be observed at the shock region because they tend to eject upward from the wall as a result of the adverse pressure gradient and flow reversal. This behavior was also observed by Pirozzoli and Grasso [1]. From a performance point of view, the rise in the boundary layer thickness and the unsteadiness of the flow downstream of the shock are both considered detrimental.

As shown in Fig. 2, velocity magnitude rapidly decrease downstream of the separation shock and strong flow mixing is observed with partial flow recovery. In addition, flow separation occurs towards the entry of the ramp, which as a by-product, results in increase in the displacement and momentum thickness, where the rapid momentum thickness increase yields a decrease in the shape factor within the separation region, as shown in Fig. 3.

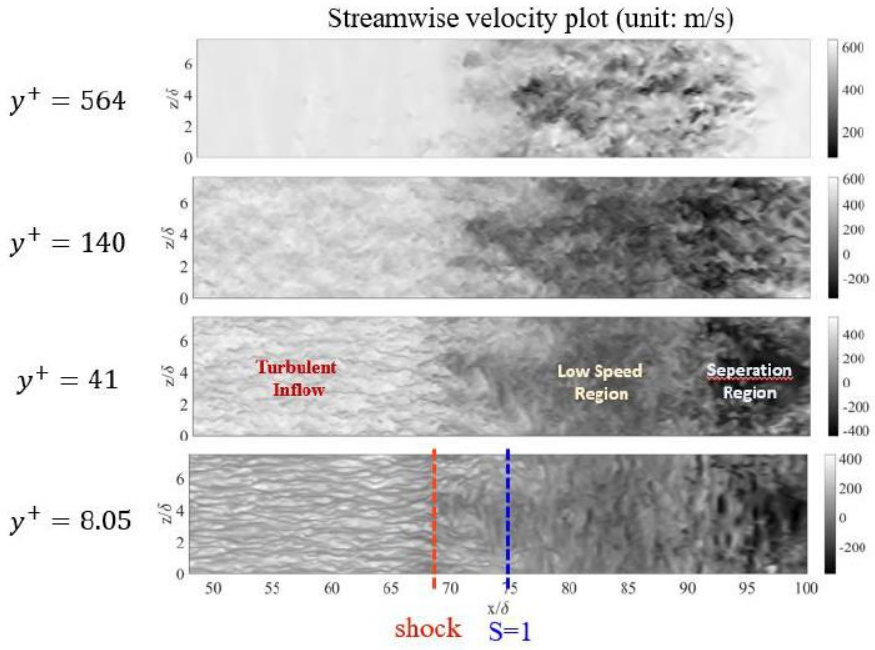

Fig. 2 Streamwise velocity contour

Loginov et al. [30] conducted a comparable investigation in their LES of a compression corner flow, in which their study encompasses an integration period of 700 time unit, potentially elucidating the pronounced spanwise disparity of various identified in their incoming turbulent boundary layer. They observed the emergence of two sets of potentially steady counter-rotating streamwise vortices near the compression corner, denoted as Görtler-like vortices. These structures exhibit resemblances to the instability mechanism observed experimentally in laminar boundary layers developing on suitably concave surfaces, as documented in the works of Görtler [31] and Floryan [32]. Consistent with the results of Loginov et al. [30], a less pronounced spanwise variation in wall pressure was evident. To assess experimental uncertainties, considerations encompass the precision of sensors, uncertainties pertaining to wind tunnel flow parameters, and geometric uncertainties including the alignment of the shock generator and the baseplate, as detailed in Willems [33].

The oil visualization conducted to assess skin friction reveals numerous low-frequency oscillations within the separation bubble. Notably, characteristic nodal and saddle points near the reattachment location are discernible. Additionally, convergence and divergence lines, indicative of vortex-induced upwash and downwash regions, underscore a substantial spanwise modulation of the flow within the specified timeframe. Although the oil visualizations imply the presence of a steady system of streamwise vortices, findings from the long-term LES distinctly indicate the streamwise vortices to be unsteady. Notably, nodal and saddle points, along with convergence and divergence lines, exhibit suppression, suggesting a diminishing spanwise modulation of the mean flow as the averaging time increases.

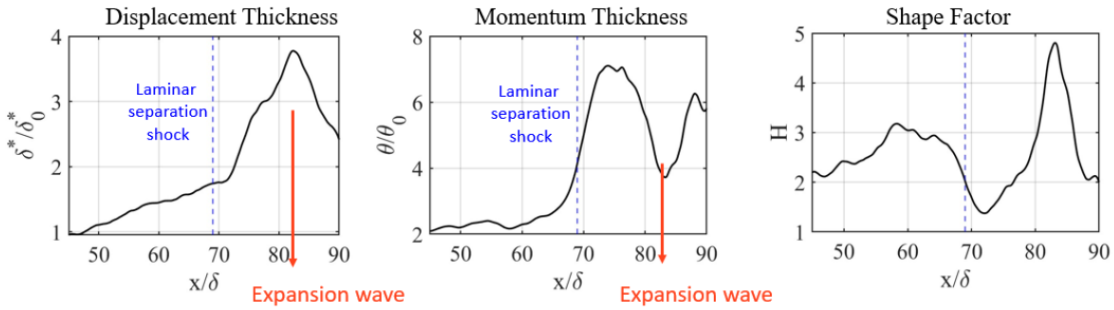

Fig. 3 Boundary layer parameters

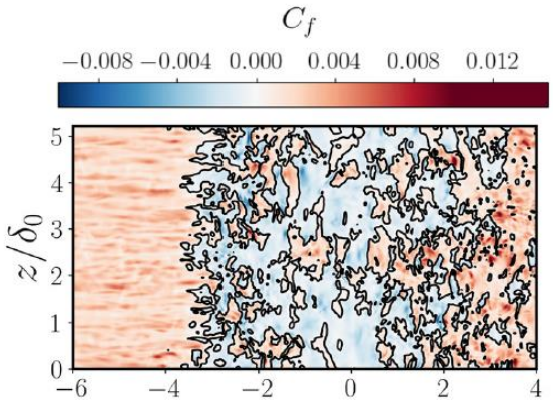

Fig. 4 Contour plot of instantaneous skin friction coefficient

The footprint of the Görtler-like structures were not found in the instantaneous skin friction coefficient, a lower ramp angle may exhibit such structures as the recirculatory motion of the separation zone becomes less active. Loginov et al. [30] have proposed a definition for the Görtler number applicable to compressible turbulent flows.

$$G_T = \frac{\theta}{0.018\delta_1}\sqrt{\frac{\theta}{|R|}} \cdot \mathrm{sgn}(R).$$

In this context, δ_1, θ, and R represent the displacement thickness, momentum thickness, and the streamline curvature radius of the mean flow, respectively. It should be noted that the aforementioned expression has been adjusted to account for both convex and concave curvature. Smits and Dussauge [34] have established a lower threshold for the curvature parameter, beyond which the onset of longitudinal vortices is anticipated. Specifically, this threshold is reported to be approximately $\delta_1/R \sim 0.03$ for a Mach number of 3. In laminar flow, the critical Görtler number is noted as $G_T = 0.58$ [31]. Both thresholds are notably surpassed within a localized zone near the separation point, as well as along an extensive region at reattachment. While the applicability of such stability criteria to turbulent flow remains uncertain, the substantial values observed within the reattachment region, persisting across a considerable streamwise extent of $11\delta_1$, suggest centrifugal instability as a plausible mechanism for the generation of Görtler-like vortices.

Fig. 5 depicts pressure profiles at different streamwise stations, revealing pressure amplification above the boundary layer edge. Analysis indicates a high-density gradient region within the free shear layer, leading to increased density and subsequent pressure elevation in this zone. Near the wall, where elevated temperatures generate a relatively high-pressure zone, a local pressure minimum emerges. This phenomenon aligns with findings reported by Yu et al. [35].

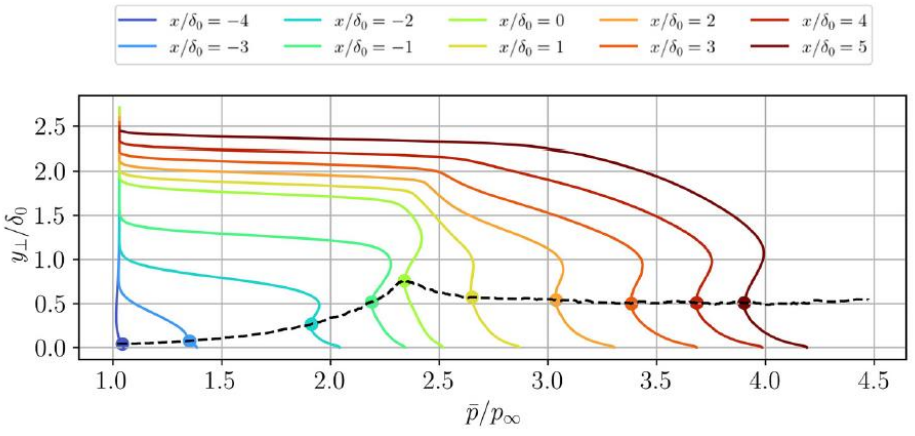

Fig. 5 Mean pressure amplification at various streamwise stations

5. Conclusion

The rapid changes in the boundary layer characteristics due to the flow separation at the interaction zone with the SBLI is an area of insufficient understanding that requires a detailed study using DNS data to reveal its primary driver that alters the pressure profile subsequent to the interaction zone compared to the upstream conditions. A seemingly feasible existence of Görler structures and the augmented level of turbulent kinetic energy within the core of the interaction zone and posterior region is organically coupled to the pressure amplification which could reveal a possible driving mechanism for the low-frequency motion of the shock.

References

1. Pirozzoli, S., Grasso, F.: Direct numerical simulation of impinging shock wave/turbulent boundary layer interaction at M = 2.25. Phys. Fluids. 18, 065113 (2006)
2. Touber, E., Sandham, ND.: Large-eddy simulation of low-frequency unsteadiness in a turbulent shock induced separation bubble. Theor. Comput. Fluid Dyn. 23, 79–107 (2009)
3. Touber, E., Sandham, ND.: Low-order stochastic modelling of low-frequency motions in reflected shockwave/boundary-layer interactions. J. Fluid Mech. 671, 417–65 (2011)
4. Priebe, S., Wu, M., Martin, M.P.: Direct numerical simulation of a reflected-shock-wave/turbulent-boundary-layer interaction. AIAA J. 47(5) (2009)
5. Bookey, P., Wyckham, C., Smits, A.: Experimental investigations of Mach 3 shock-wave turbulent boundary layer interactions. AIAA Paper. 2005-4489 (2005)
6. Pasquariello, V., Hickel, S., Adams, N.A.: Unsteady effects of strong shock-wave/boundary-layer interaction at high Reynolds number. J. Fluid Mech. 823, 617–657 (2017)
7. Nichols, J.W., Larsson, J., Bernardini, M., Pirozzoli, S.: Stability and modal analysis of shock/boundary layer interactions. Theor. Comput. Fluid Dyn. 31(1), 33–50 (2016)
8. Dolling, D.S., Or, C.T.: Unsteadiness of the shock wave structure in attached and separated compression ramp flows. Exp. Fluids. 3(1), 24–32 (1985)
9. Ringuette, M.J., Bookey, P.B., Wyckham, C., Smits, A.: Experimental study of a Mach 3 compression ramp interaction at Re_D 2400. AIAA J. 47(2), 373–385 (2009)
10. Andreopoulos, J., Muck, K.C.: Some new aspects of the shock-wave/boundary-layer interaction in compression-ramp flows. J. Fluid Mech. 180, 405–428 (1987)
11. Erengil, M.E., Dolling, D.S.: Physical causes of separation shock unsteadiness in shock-wave/turbulent boundary layer interactions. AIAA Paper. 93–3134 (1993)
12. Adams, N.A.: Direct simulation of the turbulent boundary layer along a compression ramp at M = 3 and Re_D = 1685. J. Fluid Mech. 420, 47–83 (2000)
13. Ünalmis, O., Dolling, D.: Decay of wall pressure field and structure of a Mach 5 adiabatic turbulent boundary layer. In Fluid Dynamics Conference, Reston, Virginia. AIAA (1994)
14. Beresh, S.J., Clemens, N.T., Dolling, D.S.: Relationship between upstream turbulent boundary-layer velocity fluctuations and separation shock unsteadiness. AIAA J. 40, 2412–2422 (2002)
15. Ganapathisubramani, B., Clemens, N.T., Dolling, D.S.: Low-frequency dynamics of shock-induced separation in a compression ramp interaction. J. Fluid Mech. 636, 397–425 (2009)
16. Wu, M., Martin, M.P.: Analysis of shock motion in shockwave and turbulent boundary layer interaction using direct numerical simulation data. J. Fluid Mech. 594, 71–83 (2008)
17. Humble, R.A., Elsinga, G.E., Scarano, F., Van Oudheusden, B.W.: Three-dimensional instantaneous structure of a shock wave/turbulent boundary layer interaction. J. Fluid Mech. 622, 33–62 (2009)

18. Pirozzoli, S., Larsson, J., Nichols, J.W., Morgan, B.E., Lele, S.K.: Analysis of unsteady effects in shock/boundary layer interactions. In Proceedings of the 2010 CTR Summer Program. Center of Turbulence Research (2010)
19. Dolling, D.S., Erengil, M.E.: Unsteady wave structure near separation in a Mach 5 compression ramp interaction. AIAA J. 29, 728–735 (1991)
20. Thomas, F.O., Putnam, C.M., Chu, H.C.: On the mechanism of unsteady shock oscillation in shock wave/turbulent boundary layer interactions. Exp. Fluids. 18(1), 69–81 (1994)
21. Dupont, P., Haddad, C., Debieve, J.F.: Space and time organization in a shock-induced separated boundary layer. J. Fluid Mech. 559, 255–277 (2006)
22. Piponniau, S., Dussauge, J.P., Debieve, J.F., Dupont, P.: A simple model for low frequency unsteadiness in shock-induced separation. J. Fluid Mech. 629, 87 (2009)
23. Plotkin, K.J.: Shock wave oscillation driven by turbulent boundary-layer fluctuations. AIAA J. 13(8), 1036–1040 (1975)
24. Clemens, N.T., Narayanaswamy, V.: Shock/turbulent boundary layer interactions: review of recent work on sources of unsteadiness. 39th AIAA Fluid Dynamics Conference, Reston, Virginia, 1–25. AIAA (2009)
25. Souverein, L.J., Dupont, P., Debieve, J.F., Dussauge, J.P., Van Oudheusden, B.W., Scarano, F.: Effect of interaction strength on unsteadiness in turbulent shock-wave induced separations. AIAA J. 48(7), 1480–1493 (2010)
26. Visbal, M.R., Gaitonde, D.V.: High-order-accurate methods for complex unsteady subsonic flows. AIAA J. 37(10), 1231-1239 (1999)
27. Kawai, S., Lele, S.K.: Localized artificial diffusivity scheme for discontinuity capturing on curvilinear meshes. Journal of Computational Physics. 227(22), 9498-9526 (2008)
28. Porter, K.M., Poggie, J.: Selective upstream influence on the unsteadiness of a separated turbulent compression ramp flow. Physics of Fluids. 31(1), 016104 (2019)
29. Kang, Y. and Lee, S.: Direct numerical simulation of turbulence amplification in a strong shock-wave/turbulent boundary layer interaction. Physics of Fluids. 36(1), 016127 (2024)
30. Loginov, M.S., Adams, N.A., Zheltovodov, A.A.: Large-eddy simulation of shockwave/turbulent-boundary-layer interaction. J. Fluid Mech. 565, 135 (2006)
31. Görtler, H.: Instabilität laminarer Grenzschichten an konkaven Wänden gegenüber gewissen dreidimensionalen Störungen. Z. Angew. Math. Mech. 21(4), 250–252 (1941)
32. Floryan, J.M.: On the Görtler instability of boundary layers. Prog. Aerosp. Sci. 28(3), 235–271 (1991)
33. Willems, S.: Strömung-Struktur-Wechselwirkung in Überschallströmungen. PhD thesis. German Aerospace Center (DLR), (2016)
34. Smits, A., Dussauge, J.P.: Turbulent shear layers in supersonic flow. Springer (2006)
35. Yu, M., Sun, D., Zhou, Q., Liu, P., Yuan, X.: Coherent structures and turbulent model refinement in oblique shock/hypersonic turbulent boundary layer interactions. Physics of Fluids. 35, 086125 (2023)